



OPEN

Associations between the gut microbiome and fatigue in cancer patients

Joud Hajjar^{1,2,7}, Tito Mendoza^{3,7}, Liangliang Zhang^{4,7}, Siqing Fu⁵, Sarina A. Piha-Paul⁵, David S. Hong⁵, Filip Janku⁵, Daniel D. Karp⁵, Alexej Ballhausen⁵, Jing Gong⁵, Abdulrazzak Zarifa⁵, Christine B. Peterson⁴, Funda Meric-Bernstam⁵, Robert Jenq^{6,8} & Aung Naing^{5,8}✉

Fatigue is the most prevalent symptom of cancer and its treatments. Changes in the intestinal microbiome have been identified in chronic fatigue syndrome and other neuropsychiatric disorders, and cancer patients. However, the association between intestinal microbiome and fatigue in patients with advanced cancers has not been evaluated. Understanding the connection between intestinal microbiome and fatigue will provide interventional and therapeutic opportunities to manipulate the microbiome to improve fatigue and other patients' reported outcomes. In this project, we aimed to identify associations between microbiome composition and fatigue in advanced cancer patients. In this cross-sectional observational study at a tertiary cancer care center, we included 88 patients with advanced, metastatic, unresectable cancers who were in a washout period from chemotherapy. We measured fatigue using the MD Anderson Symptom Inventory—Immunotherapy fatigue score, and used 16srRNA to analyze intestinal microbiome. Using correlation analysis we found that *Eubacterium hallii* was negatively associated with fatigue severity scores ($r = -0.30$, $p = 0.005$), whereas *Cosenzaea* was positively associated with fatigue scores ($r = 0.33$, $p = 0.0002$). We identified microbial species that exhibit distinct composition between high-fatigued and low-fatigued cancer patients. Further studies are warranted to investigate whether modulating the microbiome reduces cancer patients' fatigue severity and improves their quality of life.

Fatigue is one of the most common symptoms of cancer, and its treatment. Having fatigue has been associated with worse cancer outcomes^{1–6}. The interaction between microbial communities and the host (directly via microbial metabolites or indirectly via the immune system) supplies the central nervous system with real-time information about the environment⁷ and connects the emotional and cognitive centers of the brain with peripheral intestinal functions⁸.

Multiple studies have shown that the intestinal microbiome of cancer patients is different from that of patients without cancer. In addition, gut microbial dysbiosis prior to radiation therapy may predict fatigue in cancer patients⁹, and chemoradiotherapy can influence colorectal cancer patients' intestinal microbiome composition and contribute to fatigue¹⁰.

Fatigue is the most prevalent and pervasive symptom caused by cancer and its treatments. Although commendable efforts have been made to diagnose cancer-related fatigue, the precise cause of fatigue in cancer patients remain elusive and treatment is moderately effective, at best^{1,4,11–14}. Given recent research showing that among these patients, fatigue reduces quality of life and increases mortality^{2,5,14}, understanding the mechanism(s) of cancer-related fatigue are imperative to improve both patient experience and outcomes.

Therefore, we conducted a retrospective study of fatigue in patients with advanced cancer that lead to identification of associations between microbiota parameters and fatigue severity in cancer patients. Identifying

¹Department of Pediatrics, Baylor College of Medicine, Houston, TX, USA. ²The William T. Shearer Center for Human Immunobiology, Texas Children's Hospital, Houston, TX, USA. ³Department of Symptom Research, The University of Texas MD Anderson Cancer Center, Houston, TX, USA. ⁴Department of Biostatistics, The University of Texas MD Anderson Cancer Center, Houston, TX, USA. ⁵Department of Investigational Cancer Therapeutics, Unit 0455, The University of Texas MD Anderson Cancer Center, 1515 Holcombe Blvd, Houston, TX 77030, USA. ⁶Department of Genomic Medicine, The University of Texas MD Anderson Cancer Center, Houston, TX, USA. ⁷These authors contributed equally: Joud Hajjar, Tito Mendoza and Liangliang Zhang. ⁸These authors jointly supervised this work: Robert Jenq and Aung Naing. ✉email: anaing@mdanderson.org

intestinal microbiome features that are associated with fatigue in cancer patients may improve our understanding of the mechanisms underlying fatigue and lead to the development of therapeutic approaches targeting the microbiome to prevent or reduce fatigue in these patients.

Methods

Patients. Patients were recruited from MD Anderson's Department of Investigational Cancer Therapeutics between February 28, 2017 and January 4, 2018. Eligible patients were at least 18 years old, able to speak English, and had pathological diagnoses of advanced, metastatic, unresectable cancers. Patients had to be off antibiotics for at least 30 days before enrollment. Patients were excluded if clinical research staff believed that they did not understand the intent of the study or could not complete the symptom assessment measure. Patients' clinical and demographic data were obtained by review of their electronic medical records including cancer diagnosis, prior use of antibiotics, probiotics, medications (including antidepressants), neuropsychiatric disorders, gastrointestinal disease, and prior anti-cancer treatment. The patients underwent protocol-required wash out period before enrollment, which is typically 4 weeks or 5 half-lives of the prior therapy.

Fatigue measurement. Fatigue was assessed using the MD Anderson Symptom Inventory (MDASI)-immunotherapy module (MDASI-Immunotherapy), which has been validated for the assessment of 20 symptoms, including seven immunotherapy-specific items and six interference items¹⁵. Patients completed the module before they started immunotherapy and rated their symptoms and interference on a scale of 0–10 (0 = no symptom or no interference, 10 = worst symptom imaginable or complete interference). Using responses to the fatigue item, we categorized patients as having low fatigue (scores of 0–4) or high fatigue (scores of 5–10). The MDASI-Immunotherapy for early phase trials (EPT) has been shown to be valid and reliable¹⁵. In addition, it has been shown that the fatigue experience and its impact are reported along a single dimension and can be expressed as a single number¹⁶.

Stool collection and microbiome analysis. Stool samples were collected at baseline using the OMNI-gene-GUT kit (DNA Genotek, Inc.) and then stored at -80°C . Genomic bacterial DNA extraction methods were optimized to maximize the yield of bacterial DNA while keeping background amplification to a minimum. DNA extraction and bacterial 16S rRNA sequencing were performed as described previously¹⁷. Briefly, bacterial genomic DNA was extracted using the QIAamp DNA FFPE Tissue Kit (Qiagen). The 16S rDNA V4 region was amplified by polymerase chain reaction and sequenced using the MiSeq platform (Illumina). Between 4350 and 30,843 sequences were obtained for each sample (average 12,517). We have rarefied the OTU counts with a minimum of 4000 sequences across samples when calculating the Alpha Diversity, since this metric is sensitive to differences in sequencing depth. We have used the full unrarefied data for all the other downstream analyses, to avoid losing important information in the full microbiome data. To account for differences in read depth, we obtained the OTU relative abundances by scaling the OTU counts by their total counts in each sample.

As described in Wang, Y et al.¹⁸, we adopted the same pipeline to implement the microbiome analysis. VSEARCH was used for analyzing nucleotide sequences¹⁹. Paired-end reads were merged, de-replicated, and sorted by length and size. Sequences were then quality-controlled, error-corrected and chimera-filtered using the UNOISE algorithm to generate a preliminary list of OTUs. Both OTUs and presumed chimeras were assigned taxonomy in QIIME²⁰ using the Mothur method²¹ with the Silva database version 128²². In addition, sequences rejected by the UNOISE algorithm that matched a database entry with a perfect score were restored to generate the final list of OTUs. We utilize UNOISE3 to computationally correct for PCR errors, which come in the form of mutations and chimeras. However, UNOISE3 does not always perform perfectly, especially with chimera calling. To compensate for this, our pipeline includes a step that maps rejected sequences to the curated 16S database Silva, and those rare rejected sequences that are found have a 100% identical match in the dataset are no longer classified as noise and are added back to the other sequences.

The generated OTU table, the clustered phylogenetic tree and the assigned taxonomy were then loaded into R 3.6.1 for additional quantitative analysis. The individual OTU counts were normalized by the total OTU counts in each sample, thus the scaled OTU abundance vector sums up to one. Alpha diversity scores and UniFrac distance²³ between samples were determined using Phyloseq²⁴ and Vegan²⁵ R packages. All the other analyses, including principle coordinate analysis (PCoA), testing procedures and visualization results, were performed and produced in R.

Statistical analysis. We used statistical tests to compare demographic and clinical characteristics of the low- and high-fatigue patients. Categorical variables were evaluated using a chi-square test or a proportion test. The Mann–Whitney U test was used to compare the distributions of continuous variables between the low- and high-fatigue groups. Continuous variables were associated using Spearman correlation analyses²⁶. All tests were two-sided. *P*-values less than 0.05 were considered statistically significant.

Alpha and beta diversity were compared between groups using non-parametric tests and PCoA was used for data visualization. Unlike principal component analysis, which uses Euclidean distances, PCoA allows a choice of distance metrics, including distances designed for microbiome data such as the weighted Unifrac metric. We used three alpha-diversity metrics: the number of species observed in the sample, the Shannon index, and the Inverse Simpson index. Differential analysis of alpha diversity measures differences in the richness and evenness of microbial composition between groups of interest. Beta diversity measures the structural change in microbial compositions from one sample to another. We performed the permutational analysis of variance (PERMANOVA) to test for differences in beta diversities between groups of interest.

Characteristic	All patients (n=88)	Low-fatigue patients (n=58)	High-fatigue patients (n=30)	P-value
Median age (range), years	58.5 (22–79)	58.5 (23–78)	58 (22–79)	0.95
Sex (%)				0.2
Female	45 (51)	33 (57)	12 (40)	2.00E–05
Male	43 (49)	25 (43)	18 (60)	0.2
Race (%)				0.01
Asian	3 (3)	3 (5)	0	0.20
Black	7 (8)	2 (3)	5 (17)	0.03
White	73 (83)	52 (90)	21 (70)	0.02
Other	5 (6)	1 (2)	4 (13)	0.02
Median MDASI score (range)	3 (0–10)	2.5 (0–4)	6 (5–10)	< 0.001
ECOG score (%)				0.86
0	8 (9)	6 (10)	2 (7)	0.13
1	80 (91)	52 (90)	28 (93)	3.00E–04
Median hemoglobin level (range), gm/dL	11.9 (9–15.6)	11.9 (9.0–15.6)	11.9 (9.9–14.3)	0.98
Median albumin level (range), gm/dL	4.1 (3–4.9)	4.1 (3–4.9)	4.05 (3.2–4.7)	0.55
Median creatinine level (range), mg/dL	0.87 (0.53–1.89)	0.82 (0.53–1.89)	0.92 (0.58–1.53)	0.08

Table 1. Patient characteristics.

We categorized patients as having low fatigue (i.e., having MDASI-Immunotherapy fatigue scores of 0–4) or high fatigue (i.e., having scores of 5–10). Because microbial data are high-dimensional and heterogeneous, we need to robustly identify features that were significantly different between these two groups^{19,27}. Therefore, we used a systematic way to visualize and compare microbial data between the low- and high-fatigue groups. The “progressive permutation” method progressively permutes the grouping factor labels of the microbiome and performs multiple Mann–Whitney U tests in each scenario. The signal strengths of the top hits from the original data are compared with their performance in the permuted data; if the top hits are true positives identified from the data, a decreasing trend will emerge. Using this method, we not only evaluated the overall associations between the microbiome features and fatigue severity but also identified individual features that were robustly different between the two groups.

The fragility index is a measure of the robustness of the results of a clinical trial^{28,29}. We used a similar concept in our progressive permutation analysis to evaluate the robustness of each significant taxon. The fragility index of a variable is the minimum number of permutation steps that would change the variable’s significance to non-significance. In the present study, the larger the fragility index was, the more stable the identified taxa were. Therefore, we ranked the importance of the taxa by their fragility indices. All the statistical analyses, including alpha and beta diversity analyses, and Mann–Whitney U tests, were performed in R version 3.6.1.

Ethics approval and consent to participate. The protocol was approved by the Institutional Review Board at The University of Texas MD Anderson Cancer Center. The study was conducted in accordance with the Declaration of Helsinki and the International Conference on Harmonization Good Clinical Practice guidelines. All the study participants provided written informed consent before enrollment.

Results

The characteristics of the 88 patients (45 women and 43 men) enrolled in the study are given in Table 1. The patients’ median age was 58.5 years. Most of the patients were white (n = 73). The most frequent diagnoses were colon cancer, ovarian cancer, cervical cancer, and non-small cell lung cancer (Figure S1 in the supplementary).

MDASI-immunotherapy fatigue scores. Of the 88 patients, 58 (66%) were categorized as having low fatigue (9 had no fatigue and 49 had mild fatigue) and 30 (34%) were categorized as having high fatigue (18 had moderate fatigue and 12 had severe fatigue). The median MDASI-Immunotherapy fatigue score was 3. The mean MDASI-Immunotherapy fatigue score was 3.6 (standard deviation [SD] = 2.3). The median MDASI-Immunotherapy fatigue score was 6 for patients in the high fatigue group and was 2.5 for those in the low fatigue group.

Alpha and beta diversity comparison. The alpha diversity analysis revealed no significant differences in microbiome diversity between low- and high-fatigue patients (observed species, $p = 0.2$; Shannon index, $p = 0.57$; Inverse Simpson index $p = 0.78$; Fig. 1). The beta diversity analysis revealed no significant differences in microbial composition between low- and high-fatigue patients. Because PERMANOVA generated the insignificant results for both the weighted-UniFrac metric ($r^2 = 0.01$, $p = 0.45$, Fig. 2a) and the Bray–Curtis metric ($r^2 = 0.01$, $p = 0.40$, Fig. 2b). To compare the inter-individual variations between groups, we have added the PCoA plot with individual distances to the centroid (Fig. 2c) and the boxplot of inter-individual distances (Fig. 2d). Figure

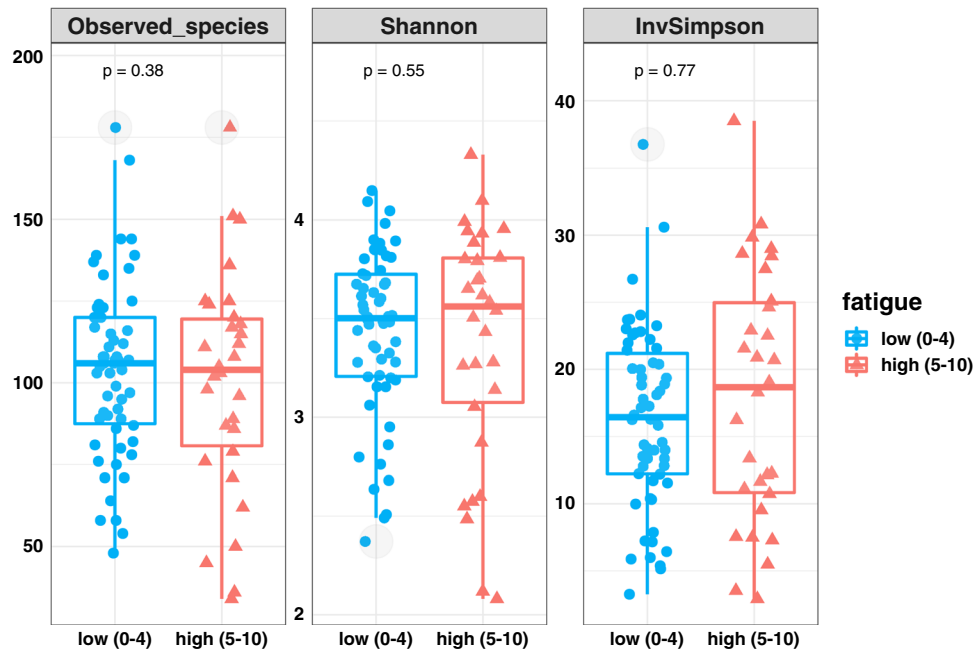


Figure 1. Box plots showing differences in alpha diversity between low- and high-fatigue patients. Each blue dot represents one patient in the low-fatigue group; each red triangle represents one patient in the high-fatigue group. The box-and-whisker plot describes the distribution of data points, including minimum, maximum, median, first quartile and third quartile. Grey shaded circles denote outliers.

c,d showed results from Bray–Curtis metric. The Tukey test concluded a nonsignificant result ($p = 0.31$). We also included the two types of plots for weighted-UniFrac metric in the supplementary (Figure S3). The Tukey test also concluded a nonsignificant result ($p = 0.51$).

Differences in the relative abundance of microbial taxa. Microbial features were agglomerated across the taxonomic levels phylum, class, order, family, genus, and species. The taxonomic compositions in low- and high-fatigue groups at phylum-class-order-family-genus levels are shown in Figure S2 (in the supplementary). Mann–Whitney U tests identified 15 of these features to be significantly differential between low- and high-fatigue groups ($p < 0.05$; Figure S4). Among the 24 features, a subgroup of 12 features (labelled in Figure S4) were identified to be robust findings based on the progressive permutation analysis. The trending curve of P-Values, the fragility indices and the effect sizes are shown in Figure S5 in the supplementary.

To verify the results, we also applied the DESeq method³⁰, with the Benjamini–Hochberg procedure used to adjust the p-values³¹. We presented the adjusted p-values in the volcano plot (Fig. 3). Eight features identified by DESeq agree with the ones identified by our Wilcoxon method. We also applied LefSe and presented the results in the barplot (Figure S6 in the supplementary). LefSe uses both p-values and LDA scores to determine hits; however, it does not adjust the p-values for multiplicity. Using the default threshold of 2 on the LDA scores³², LefSe selected 21 features in total. Eleven features identified by LefSe agree with the ones identified by our method. We have also performed indicator species analysis using the labdsv package in R. We have plotted the selected variables and their $-\log_{10}$ p-values, as shown in the supplementary (Figure S6 in the supplementary). We still found five same features that are identified by our method.

We studied and plotted the distribution across samples of these 12 features one-by-one in Fig. 4 and Figure S11 in the supplementary. *Eubacterium hallii* and *Cosenzaea* were most differential between the high- and low-fatigue groups (Fig. 4). Both of them are also identified by all the above testing procedures. Compared with the low-fatigue group, the high-fatigue group had a significantly lower abundance of *Eubacterium hallii* ($p = 0.005$; Fig. 4a) but a significantly higher abundance of *Cosenzaea* ($p = 0.0039$; Fig. 4b). The abundances of *Eubacterium hallii* and *Cosenzaea* in each patient sample grouped by fatigue severity are shown in Figures S4A and S4B in the supplementary. Correlation analysis revealed that *Eubacterium hallii* was negatively associated with fatigue severity score ($r = -0.31$, $p = 0.0026$), whereas *Cosenzaea* was positively associated with fatigue severity score ($r = 0.26$, $p = 0.014$). As the correlation analysis is mainly meant for visualization and exploration instead of inference, the p-values in the correlation analysis are not adjusted to correct for multiple testing.

We performed the Random Forest method to check the classification accuracy using the 12 selected features. We randomly split the data into 70% training set and 30% testing set. We repeated the training and testing procedure for 50 times. We have added the plot of the importance of these selected features in Figure S9 in the supplementary. It shows that the taxonomic feature “Species.Clostridium_dakarensense” has the highest importance. We performed SpiecEasi (SParse InversE Covariance Estimation for Ecological Association Inference) to infer the network structures. Compared with CCREPE and SparCC, which are focused on estimation of unconditional

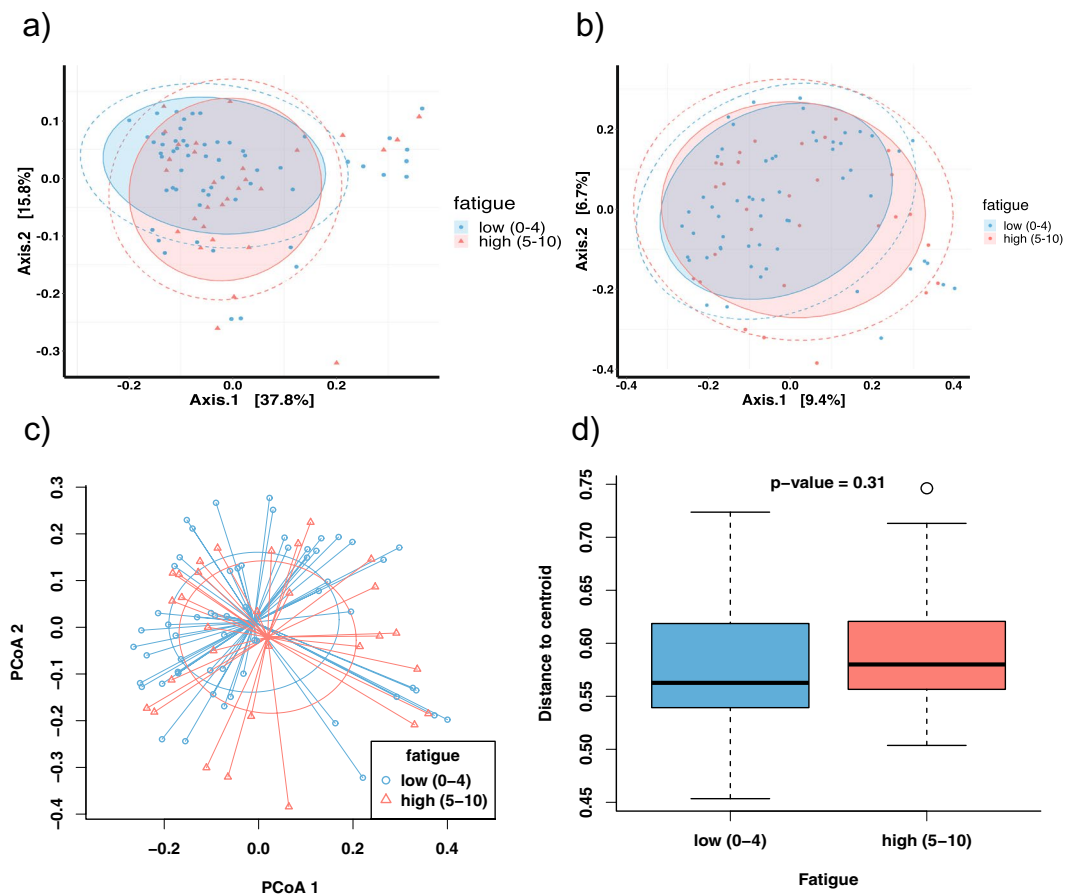


Figure 2. Results of the principal coordinate analysis (PCoA) showing differences in beta diversity between low- and high-fatigue patients. **(a)** PCoA plots using weighted-UniFrac metric. The x-axis explains 37.8% variation of the data. The y-axis explains 15.8% variation of the data. Each blue dot represents the PCoA score of one patient in the low-fatigue group; Each red triangle represents the PCoA score of one patient in the high-fatigue group. **(b)** PCoA plots using Bray-Curtis metric. The x-axis explains 9.4% variation of the data. The y-axis explains 6.7% variation of the data. The shaded ellipse denote the 80% confidence region of all the points. The dashed ellipse denote the 90% confidence region of all the points. **(c)** PCoA plot with individual distances to the centroid shows the inter-individual variations. Each blue dot represents the PCoA score of one patient in the low-fatigue group; Each red triangle represents the PCoA score of one patient in the high-fatigue group. **(d)** Boxplot of individual-centroid distances. The p-value is given by Tukey test. The box with blue color describes the distance distribution in the low fatigue group; The box with red color describes the distance distribution in the high fatigue group. **(c,d)** showed results from Bray-Curtis metric.

correlation, SpiecEasi reliably estimates a sparse inverse covariance which can model the conditional independence between microbial features³³. We have added the plot of the network at the genus level (178 features) in Figure S8 in the supplementary. When comparing the two networks, the low fatigue group network includes 285 edges, while the high fatigue group network includes 345 edges. This indicates that there are more co-occurring genera found in the high-fatigue group.

We performed Spearman correlation analysis to show the correlations between microbial abundances and clinical factors. The taxa that were resolved till genus and species levels were shown in the correlation plot (Fig. 5). The results revealed that microbiome features were not strongly correlated with clinical factors that are potentially associated with fatigue severity, including hemoglobin level, albumin level, creatinine level, Eastern Cooperative Oncology Group performance status score, number of lines of treatment, metastatic status, and age (Fig. 5). We have provided scatterplots showing correlations between *Eubacterium hallii* and fatigue severity score, and *Cosenzaea* and fatigue severity score. The figures have been included in Figure S12 of the supplementary.

Discussion

In this study, we identified possible link between microbiome composition and fatigue in patients with advanced cancers. Using the MD Anderson Symptom Inventory to score fatigue and 16S rRNA sequencing to characterize the intestinal microbiome of 88 patients with advanced, metastatic, unresectable cancer, we observed that

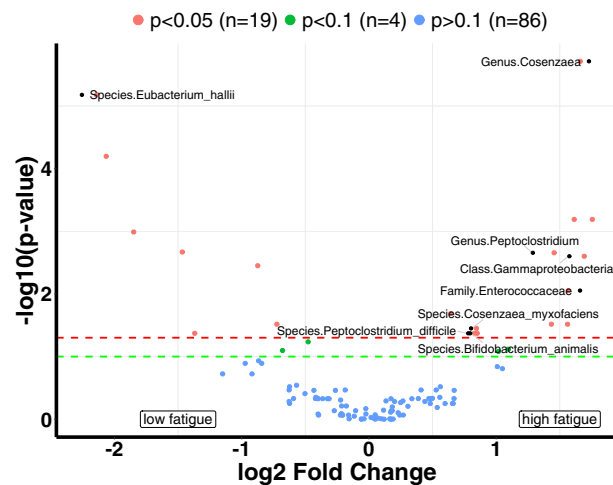


Figure 3. Volcano plot showing that, of 109 taxonomic features, 19 were significantly differential between low- and high-fatigue groups ($p < 0.05$; DESeq test with Benjamini–Hochberg procedure to adjust the p -values). Eight features identified by DESeq agree with the ones identified by our method. They were annotated with text names in the plot. The blue dot represents the features whose p -values are greater than 0.1; the green dot represents the features whose p -values are less than 0.1 and greater than 0.05; the red dot represents the features whose p -value are less than 0.05. A positive effect size indicates that the microbial feature is more abundant in high-fatigue group.

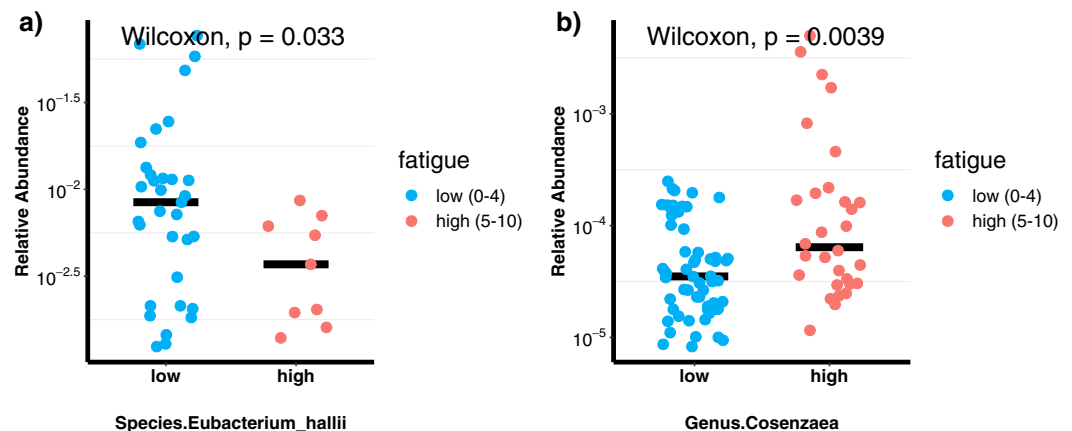


Figure 4. (a) Dot plots showing differences in relative abundance in *Eubacterium hallii* abundance between the high- and low-fatigue groups. Each blue dot represents one patient in the low-fatigue group; each red dot represents one patient in the high-fatigue group. The black bar denotes the median. (b) Dot plots showing differences in relative abundance in *Cosenzaea* abundance between the high- and low-fatigue groups. Each blue dot represents one patient in the low-fatigue group; each red dot represents one patient in the high-fatigue group. The black bar denotes the median. In both figures, we performed \log_{10} transformation of the data so that the data points are evenly distributed. The numbers on the y -axis denotes the original quantity of relative abundance, which are just the scientific format of the abundance proportions.

Eubacterium hallii was negatively associated with fatigue scores whereas *Cosenzaea* was positively associated with fatigue scores.

Eubacterium hallii, considered a key species in trophic interactions, can highly impact metabolic balance, ultimately affecting gut microbiota and host homeostasis as well as host health³⁴. In addition, *Eubacterium hallii* has been used to treat insulin resistance-related conditions, including dyslipidemia, type 1 diabetes mellitus, and Cushing syndrome, and other endocrine diseases³⁵. Together, these data suggest that *Eubacterium hallii* has a role in intestinal metabolism and immune homeostasis that might impact the gut-brain axis and fatigue.

Cosenzaea myxofaciens (previously known as *Proteus myxofaciens*), together with the genera *Proteus*, *Providencia*, and *Morganella*, belongs to the family Enterobacteriaceae within the tribe Proteae³⁶. No data on the role of *Cosenzaea* in cancer have been reported. Under favorable conditions, *Proteus* bacteria, which inhabit the environment and are present in the intestines of humans, can cause urinary tract infections, wound infections,

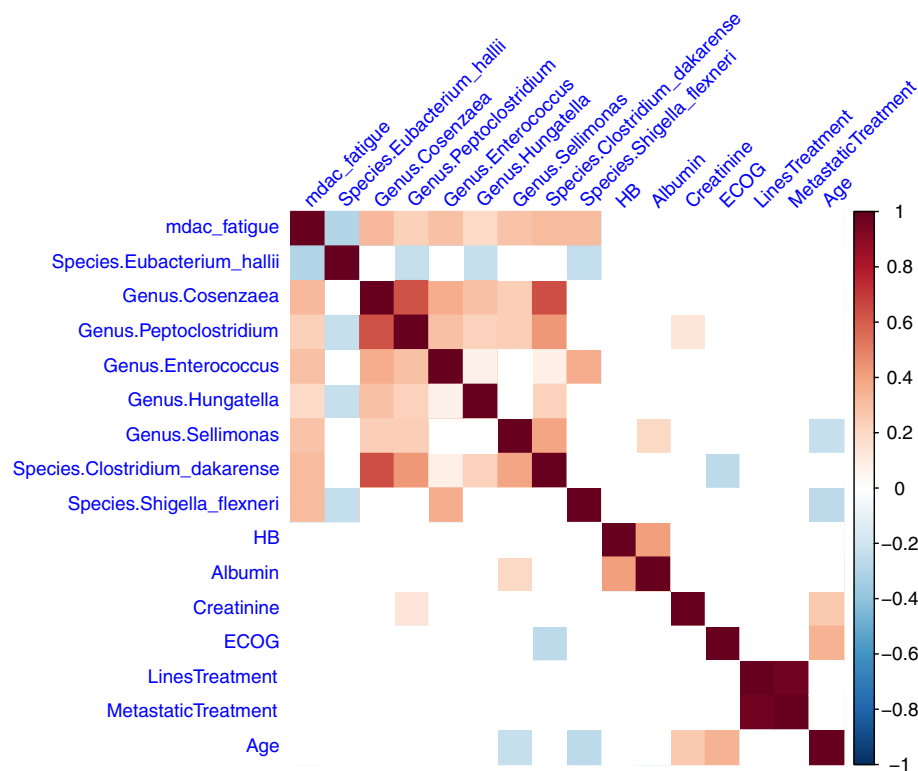


Figure 5. Results of the Spearman correlation analysis showing relationships among fatigue, selected microbiome species, and clinical measurements. The blue color indicates negative correlation while the red color indicates positive correlation. The depth of the color describes the strength of correlation. The absence of a color indicates a lack of no correlation (p -value > 0.05).

and meningitis (in neonates and infants). The increased abundance of *Cosenzaea myxofaciens* in high-fatigue cancer patients indicates a potential role of the bacteria in inducing inflammation.

Limitations

This study had a relatively small sample size, which might have precluded the identification of significant differences in the diversity of the microbiome between high- and low-fatigue patients, and across different types of cancer. In addition, six patients were on antibiotics within 1–3 months of stool sample collection, which could have affected their intestinal microbiome composition. However, recent studies have suggested that antibiotic use in the preceding 30 days is not associated with alpha diversity or dysbiosis index³⁷. The mean fatigue score in our cohort was lower than those previously reported for cancer patients receiving no treatment (4.52, SD = 3.3), patients receiving chemotherapy (5.2, SD = 2.81), and patients receiving bone marrow transplantations (5.29, SD = 2.55)³⁸. This may be explained by the good performance status our patients were required to have to meet the eligibility criteria for enrollment on clinical trials, and this might present some selection bias. However, we were able to identify a significant difference in fatigue scores (some with severe fatigue and others with mild fatigue) even among patients with good performance status. Finally, we did not have healthy controls in this study, however, we plan to collect healthy household samples in future longitudinal studies.

Conclusions

Our study shows that cancer patients experiencing different levels of fatigue can have distinct gut microbiome compositions. Given the importance of the microbiome in mucosal immunity and increasing recognition of the association between the gut-brain axis and fatigue and other symptoms, our findings highlight the need to further evaluate the microbiome in cancer patients with fatigue using longitudinal samples, and assess whether modulating the microbiome reduces cancer patients' fatigue severity and improves their quality of life.

Data availability

The datasets used and/or analyzed during the current study are available from the corresponding author on reasonable request according to available guidelines at the time of request.

Received: 15 November 2020; Accepted: 18 February 2021

Published online: 12 March 2021

References

- Bower, J. E. Cancer-related fatigue: Mechanisms, risk factors, and treatments. *Nat. Rev. Clin. Oncol.* **11**, 597–609. <https://doi.org/10.1038/nrclinonc.2014.127> (2014).
- Efficace, F. *et al.* Chronic fatigue is the most important factor limiting health-related quality of life of chronic myeloid leukemia patients treated with imatinib. *Leukemia* **27**, 1511–1519. <https://doi.org/10.1038/leu.2013.51> (2013).
- Flechtner, H. & Bottomley, A. Fatigue and quality of life: Lessons from the real world. *Oncologist* **8**(Suppl 1), 5–9 (2003).
- Stasi, R., Abriani, L., Beccaglia, P., Terzoli, E. & Amadori, S. Cancer-related fatigue: Evolving concepts in evaluation and treatment. *Cancer* **98**, 1786–1801. <https://doi.org/10.1002/cncr.11742> (2003).
- Bower, J. E. *et al.* Fatigue in breast cancer survivors: Occurrence, correlates, and impact on quality of life. *J. Clin. Oncol.* **18**, 743–753. <https://doi.org/10.1200/JCO.2000.18.4.743> (2000).
- Curt, G. A. *et al.* Impact of cancer-related fatigue on the lives of patients: new findings from the Fatigue Coalition. *Oncologist* **5**, 353–360 (2000).
- Sharon, G., Sampson, T. R., Geschwind, D. H. & Mazmanian, S. K. The central nervous system and the gut microbiome. *Cell* **167**, 915–932. <https://doi.org/10.1016/j.cell.2016.10.027> (2016).
- Carabotti, M., Scirocco, A., Maselli, M. A. & Severi, C. The gut-brain axis: Interactions between enteric microbiota, central and enteric nervous systems. *Ann. Gastroenterol.* **28**, 203–209 (2015).
- Wang, A. *et al.* Gut microbial dysbiosis may predict diarrhea and fatigue in patients undergoing pelvic cancer radiotherapy: A pilot study. *PLoS ONE* **10**, e0126312. <https://doi.org/10.1371/journal.pone.0126312> (2015).
- González-Mercado, V. J. *et al.* The role of gut microbiome perturbation in fatigue induced by repeated stress from chemoradiotherapy: A proof of concept study. *Adv. Med.* <https://doi.org/10.1155/2020/6375876> (2020).
- Xiao, C. *et al.* Fatigue is associated with inflammation in patients with head and neck cancer before and after intensity-modulated radiation therapy. *Brain Behav. Immun.* **52**, 145–152. <https://doi.org/10.1016/j.bbi.2015.10.016> (2016).
- Bower, J. E. & Lamkin, D. M. Inflammation and cancer-related fatigue: Mechanisms, contributing factors, and treatment implications. *Brain Behav. Immun.* **30**(Suppl), S48–57. <https://doi.org/10.1016/j.bbi.2012.06.011> (2013).
- Gripp, S. *et al.* Survival prediction in terminally ill cancer patients by clinical estimates, laboratory tests, and self-rated anxiety and depression. *J. Clin. Oncol.* **25**, 3313–3320. <https://doi.org/10.1200/JCO.2006.10.5411> (2007).
- Stone, P. *et al.* Fatigue in advanced cancer: A prospective controlled cross-sectional study. *Br. J. Cancer* **79**, 1479–1486. <https://doi.org/10.1038/sj.bjc.6690236> (1999).
- Mendoza, T. *et al.* Evaluating the psychometric properties of the immunotherapy module of the MD anderson symptom inventory. *J. Immunother. Cancer* <https://doi.org/10.1136/jitc-2020-000931> (2020).
- Cella, D., Lai, J. S. & Stone, A. Self-reported fatigue: One dimension or more? Lessons from the functional assessment of chronic illness therapy-fatigue (FACIT-F) questionnaire. *Support Care Cancer* **19**, 1441–1450. <https://doi.org/10.1007/s00520-010-0971-1> (2011).
- Caporaso, J. G. *et al.* Ultra-high-throughput microbial community analysis on the Illumina HiSeq and MiSeq platforms. *ISME J.* **6**, 1621–1624. <https://doi.org/10.1038/ismej.2012.8> (2012).
- Wang, Y. *et al.* Fecal microbiota transplantation for refractory immune checkpoint inhibitor-associated colitis. *Nat. Med.* **24**, 1804–1808. <https://doi.org/10.1038/s41591-018-0238-9> (2018).
- Rognes, T., Flouri, T., Nichols, B., Quince, C. & Mahe, F. VSEARCH: A versatile open source tool for metagenomics. *PeerJ* **4**, e2584. <https://doi.org/10.7717/peerj.2584> (2016).
- Caporaso, J. G. *et al.* QIIME allows analysis of high-throughput community sequencing data. *Nat. Methods* **7**, 335–336. <https://doi.org/10.1038/nmeth.f.303> (2010).
- Schloss, P. D. *et al.* Introducing mothur: Open-source, platform-independent, community-supported software for describing and comparing microbial communities. *Appl. Environ. Microbiol.* **75**, 7537–7541. <https://doi.org/10.1128/AEM.01541-09> (2009).
- Schloss, P. D. *Silva reference files*, https://mothur.org/wiki/silva_reference_files/#release-128 (2019).
- Lozupone, C. & Knight, R. UniFrac: A new phylogenetic method for comparing microbial communities. *Appl. Environ. Microbiol.* **71**, 8228–8235. <https://doi.org/10.1128/AEM.71.12.8228-8235.2005> (2005).
- McMurdie, P. J. & Holmes, S. phyloseq: An R package for reproducible interactive analysis and graphics of microbiome census data. *PLoS ONE* **8**, e61217. <https://doi.org/10.1371/journal.pone.0061217> (2013).
- Oksanen, J., Kindt, R., Legendre, P., O'Hara, B., Stevens, M.H.H. & Oksanen, M.J. *The vegan package. Community ecology package*, <http://CRAN.Rproject.org/package=vegan> (2007).
- Bolboaca, S. & Jäntschi, L. Pearson versus Spearman, Kendall's Tau correlation analysis on structure-activity relationships of biologic active compounds. *Leonardo J. Sci.* **9**, 2 (2006).
- Edgar, R. C. UPARSE: Highly accurate OTU sequences from microbial amplicon reads. *Nat. Methods* **10**, 996–998. <https://doi.org/10.1038/nmeth.2604> (2013).
- Walsh, M. *et al.* The statistical significance of randomized controlled trial results is frequently fragile: A case for a Fragility Index. *J. Clin. Epidemiol.* **67**, 622–628. <https://doi.org/10.1016/j.jclinepi.2013.10.019> (2014).
- Feinstein, A. R. The unit fragility index: An additional appraisal of “statistical significance” for a contrast of two proportions. *J. Clin. Epidemiol.* **43**, 201–209. [https://doi.org/10.1016/0895-4356\(90\)90186-s](https://doi.org/10.1016/0895-4356(90)90186-s) (1990).
- Anders, S. & Huber, W. Differential expression analysis for sequence count data. *Genome Biol.* **11**, R106. <https://doi.org/10.1186/gb-2010-11-10-r106> (2010).
- Thissen, D., Steinberg, L. & Kuang, D. Quick and easy implementation of the Benjamini-Hochberg procedure for controlling the false positive rate in multiple comparisons. *J. Educ. Behav. Stat.* **27**, 77–83. <https://doi.org/10.3102/10769986027001077> (2002).
- Segata, N. *et al.* Metagenomic biomarker discovery and explanation. *Genome Biol.* **12**, R60. <https://doi.org/10.1186/gb-2011-12-6-r60> (2011).
- Kurtz, Z. D. *et al.* Sparse and compositionally robust inference of microbial ecological networks. *PLoS Comput. Biol.* **11**, e1004226. <https://doi.org/10.1371/journal.pcbi.1004226> (2015).
- Engels, C., Ruscheweyh, H. J., Beerenwinkel, N., Lacroix, C. & Schwab, C. The common gut microbe eubacterium hallii also contributes to intestinal propionate formation. *Front. Microbiol.* **7**, 713. <https://doi.org/10.3389/fmicb.2016.00713> (2016).
- Olveira, G. & Gonzalez-Molero, I. An update on probiotics, prebiotics and symbiotics in clinical nutrition. *Endocrinol. Nutr.* **63**, 482–494. <https://doi.org/10.1016/j.endonu.2016.07.006> (2016).
- Giammanco, G. M. *et al.* Phylogenetic analysis of the genera Proteus, Morganella and Providencia by comparison of rpoB gene sequences of type and clinical strains suggests the reclassification of Proteus myxofaciens in a new genus, Cosenzaea gen. nov., as Cosenzaea myxofaciens comb. nov. *Int J Syst Evol Microbiol* **61**, 1638–1644. <https://doi.org/10.1099/ijs.0.021964-0> (2011).
- Jorgensen, S. F. *et al.* Altered gut microbiota profile in common variable immunodeficiency associates with levels of lipopolysaccharide and markers of systemic immune activation. *Mucosal Immunol.* **9**, 1455–1465. <https://doi.org/10.1038/mi.2016.18> (2016).
- Cleeland, C. S. *et al.* Assessing symptom distress in cancer patients: The M.D. Anderson symptom inventory. *Cancer* **89**, 1634–1646 (2000).

Acknowledgements

We thank the patients and their families and caregivers for participating in the study. We also thank Joseph A. Munch, Sr. Scientific Editor at MD Anderson, for providing editorial assistance. We have uploaded the raw sequencing data to the MG-RAST website. Researchers can download the data from the link <https://www.mg-rast.org/mgmain.html?mgpage=project&project=mgp97329>.

Author contributions

J.H. contributed to concept and design, data analysis and interpretation, drafting the manuscript, critical revision of the manuscript, and final approval; T.M. contributed to the data acquisition, data analysis and interpretation, drafting the manuscript, critical revision of the manuscript, and final approval; L.Z. contributed to data analysis and interpretation, drafting the manuscript, critical revision of the manuscript, and statistical analysis; S.F. contributed to data acquisition, critical review and final approval of the manuscript; S.A.P.-P. contributed to data acquisition, critical review and final approval of the manuscript; D.S.H. contributed to data analysis and interpretation, critical revision of the manuscript, technical, administrative, and material support, and final approval; F.J. contributed to data acquisition, critical review and final approval of the manuscript; D.D.K. contributed to data acquisition, critical review and final approval of the manuscript; A.B. contributed to the data collection and final approval; J.G. contributed to the data and acquisition and technical, administrative, and material support; A.Z. contributed to the data acquisition and data analysis and interpretation; C.P. contributed to critical revision of the manuscript, statistical analysis, and final approval; F.M.-B. contributed to study design, data interpretation, critical review and final approval of the manuscript; R.J. contributed to data analysis and interpretation, critical revision of the manuscript, and final approval; A.N. contributed to concept and design, data acquisition, data analysis and interpretation, drafting the manuscript, critical revision of the manuscript, technical, administrative, and material support and final approval.

Funding

Support provided, in part, by the Biostatistics Resource Group and the Assessment, Intervention and Measurement (AIM) Shared Resource through a Cancer Center Support Grant (CA16672, PI: P. Pisters, MD Anderson Cancer Center) and by Clinical Translational Science Award 1UL1 TR003167. TM was supported by NIH/NCI R01CA242565.

Competing interests

JH reports research support from Immune Deficiency Foundation, Jeffery Modell Foundation and Chao Physician-Scientist, and Baxalta and has served on an advisory board for Takeda, CSL, Behring, Horizon, and Pharming, outside the submitted work; SF reports clinical trial research support from AstraZeneca, Abbisko, Anaeropharma Science, Arrien Pharmaceuticals, BeiGene, BioAtla, LLC, Boehringer Ingelheim, Eli Lilly, Hookipa Biotech, Huya Bioscience International, IMV, Inc., Innovent Biologics, Co., Ltd., Lyvgen Biopharm, Co., Ltd., MacroGenics, Medivir AB, Millennium Pharmaceuticals, Inc., Nerviano Medical Sciences, NeuPharma, Inc., NIH/NCI, Novartis, OncoMed Pharmaceuticals, Parexel International, LLC, Sellas Life Sciences Group, Soricimed Biopharma, Inc., Tolero Pharmaceuticals, outside the submitted work, grants from NIH/NCI; SAP-P reports grants from AbbVie, Inc., ABM Therapeutics, Inc., Acepodia, Inc., Alkermes, Inc., Aminex Therapeutics, Amphivena Therapeutics, Inc., BioMarin Pharmaceutical, Inc., Boehringer Ingelheim, Bristol Myers Squibb, Chugai Pharmaceutical Co., Daiichi Sankyo, Inc., Eli Lilly, Five Prime Therapeutics, Genmab A/S, GlaxoSmithKline, Helix BioPharma Corp., Incyte Corp., Jacobio Pharmaceuticals Co., Ltd, Medimmune, LLC, Medivation, Inc., Merck Sharp and Dohme Corp., Novartis Pharmaceuticals, Pieris Pharmaceuticals, Inc., Pfizer, Principia Biopharma, Inc., Puma Biotechnology, Inc., Rapt Therapeutics, Inc., Seattle Genetics, Taiho Oncology, Tesaro, Inc., Transthera Bio, and NCI/NIH Core Grant, outside the submitted work; DSH reports research/grant funding from Abbvie, Adaptimmune, Amgen, Astra-Zeneca, BMS, Daiichi-Sankyo, Eisai, Fate Therapeutics, Genmab, Ignyta, Kite, Kyowa, Lilly, Medimmune, Merck, Merrimack, Mirati, MIRNA, Molecular Templates, Mologen, NCI-CTEP, Novartis, Pfizer; personal fees from Axiom, Baxter, GLG, Group H, Guidepoint Global, Janssen, Medscape, Numab, Trieza Therapeutics; research/grant funding and personal fees from Bayer, Genentech, Infinity, LOXO, Seattle Genetics, Takeda; and other from Molecular Match, OncoResponse, Presagia Inc, during the conduct of the study; FJ reports grants and research funding from Novartis, Genentech, BioMed Valley Discoveries, Plexxikon, Piquor, Symphogen, Bayer, and Fujifilm Corporation, Astex, Asana, Astellas, Agios, Proximagen, Bristol-Myers Squibb, and Upsher-Smith Laboratories, research funding & SAB from Deciphera, SAB from IFM Therapeutics, Synlogic, Gaurdant Health, Ideaya, and PureTech Health, and services as paid consultant & ownership interests in Trovogene, and paid consultant in Immunomet, Sotio, and Jazz Pharmaceuticals, outside the submitted work; FM-B reports grants from Aileron, AstraZeneca, Bayer Healthcare Pharmaceutical, Calithera Biosciences Inc., Curis Inc., CytomX Therapeutics Inc., Daiichi Sankyo Co. Ltd., Guardant Health Inc., Millennium Pharmaceuticals, Novartis, Taiho Pharmaceutical Co.; personal fees for advisory from Seattle Genetics Inc., Immunomedics, Inflection Biosciences, Mersana Therapeutics, Silverback Therapeutics, Spectrum Pharmaceuticals, Zentalis; personal fees from Aduro, BioTech Inc, Alkermes, F. Hoffman-La Roche Ltd, IBM Watson, Jackson Laboratory, Kolon Life Science, OrigiMed, PACT Pharma, Parexel International, Pfizer Inc., Samsung Bioepis, Tyra Biosciences, Xencor, Zymeworks; personal fees for travel related from Beth Israel Deaconess Medical Center, grants and personal fees for Consulting from Genentech, Debio, and eFFECTOR Therapeutics; personal fees for consulting and advisory committee from Seattle Genetics Inc., personal fees for advisory and grants Puma Biotechnology Inc.; grants from Chugai Biopharmaceuticals, Mayo Clinic, and Rutgers Cancer Institute of New Jersey outside the submitted work; RJ reports personal fees from Kaleido Biosciences, Seres Therapeutics, Merck, Proclata Bioscience, MaaT Pharma, MicroBiomeDX, Karius, Ziopharm Oncology, and holds a patent with Seres

Therapeutics, outside the submitted work; AN reports research support and non-financial support from Merck Sharp & Dohme Corp., grants from NCI/NIH, research support from The University of Texas MD Anderson Cancer Center, during the conduct of the study; grants from NCI, research support from EMD Serono, MedImmune, Healios Onc. Nutrition, Atterocor, Amplimmune, ARMO BioSciences, Karyopharm Therapeutics, Incyte, Novartis, Regeneron, Merck, Bristol Myers Squibb, Pfizer, CytomX Therapeutics, Neon Therapeutics, Calithera BioSciences, TopAlliance BioSciences, Eli Lilly, Kymab, Arcus, and PsiOxus, A non-financial support for travel and accommodation from ARMO BioSciences, and has served as an advisory board member for Novartis, Kymab, Genome & Company, and CytomX Therapeutics outside the submitted work. TM, LZ, DDK, AB, JG, AZ, CP declare no competing interests.

Additional information

Supplementary Information The online version contains supplementary material available at <https://doi.org/10.1038/s41598-021-84783-9>.

Correspondence and requests for materials should be addressed to A.N.

Reprints and permissions information is available at www.nature.com/reprints.

Publisher's note Springer Nature remains neutral with regard to jurisdictional claims in published maps and institutional affiliations.



Open Access This article is licensed under a Creative Commons Attribution 4.0 International License, which permits use, sharing, adaptation, distribution and reproduction in any medium or format, as long as you give appropriate credit to the original author(s) and the source, provide a link to the Creative Commons licence, and indicate if changes were made. The images or other third party material in this article are included in the article's Creative Commons licence, unless indicated otherwise in a credit line to the material. If material is not included in the article's Creative Commons licence and your intended use is not permitted by statutory regulation or exceeds the permitted use, you will need to obtain permission directly from the copyright holder. To view a copy of this licence, visit <http://creativecommons.org/licenses/by/4.0/>.

© The Author(s) 2021